REGULAR PAPER

Molecular chaperone αB-crystallin regulates the dynamic stability of focal adhesion under mechanical stress conditions

Japanese Journal of Applied Physics **59**, SDDE03 (2020) **REGULAR PAPER**
https://doi.org/**10.7567/1347-4065/ab65aa**

Molecular chaperone αB-crystallin regulates the dynamic stability of focal adhesion under mechanical stress conditions

Saaya Hayasaki[1], Yasuomi Sasai[2], Masaki Imayasu[2], Miho Shimizu[1], Soichiro Fujiki[3], Keiji Naruse[4], Toshiyuki Watanabe[5], and Yoriko Atomi[1*]

[1]*Material Health science Laboratory, Graduate School of Engineering, Tokyo University of Agriculture and Technology, Koganei, Tokyo, 184-8588, Japan*
[2]*Menicon Co., Ltd., Nagoya, Aichi, 452-0805, Japan*
[3] *Department of Physiology and Biological Information, Dokkyo Medical University, Mibu, Tochigi, 321-0293, Japan*
[4]*Department of Cardiovascular Physiology, Graduate School of Medicine, Dentistry and Pharmaceutical Sciences, Okayama University, Shikata, Okayama, 700-8558, Japan*
[5]*Division of Applied Chemistry, Graduate School of Engineering, Tokyo University of Agriculture and Technology, Koganei, Tokyo, 184-8588, Japan*

[*]E-mail: yatomi@cc.tuat.ac.jp

Received August 19, 2019; revised December 17, 2019; accepted December 26, 2019; published online January 22, 2020

Resilience to stretch stress is an important characteristic that helps maintain cell adhesion and consequently, human health. This study aimed to elucidate the underlying mechanism of adaptation to stretch stress regulated by the molecular chaperone αB-crystallin. Three rat myoblast L6 cell lines, wild type (L6-WT), αB-crystallin knock down (L6-KD), and αB-crystallin overexpressing (L6-OE) cells were used. Muscle cells are less motile because they are specialized for contraction. Forced stretch stress was given to the three cell lines on a soft adhesive sheet, and we found that L6-OE cells showed the highest resilience to stretch stress and the least motility compared to other cell lines. Conversely, L6-KD cells showed the least resilience to stretch stress. Vinculin staining showed that total focal adhesion (FA) size and area of L6-OE cells were significantly larger than those of other cell types. Thus αB-crystallin in myoblast cells contributes the resilience of FA stability during stretch stress.

1. Introduction

Cells in multicellular organisms are always exposed to mechanical stress, such as tension,[1)] shear stress,[2)] hydrostatic pressure,[3)] vibration,[4)] and gravity.[5)] To maintain cell adhesion, cells have a cytoskeletal structure connected to focal adhesion (FA) that produces tension, and cell survival is dynamically controlled. However, the mechanism of FA resilience is unknown. Since cells die once they are detached from the substrate, cell resilience to the collapse of cytoskeleton and FA during stretch is essential for cell survival.

Stress proteins, also called heat shock proteins (HSPs) and/or molecular chaperones, are hypothesized to be involved in FA adaptation. HSPs respond to various stresses and function as molecular chaperones to assist in the conformational folding or refolding, and assembly or disassembly of other protein structures.[6,7)] Such capabilities for examples protect cells from toxic oligomers of amyloid-peptides in Alzheimer's disease.[8)] Studies have shown that molecular chaperones support adaptive evolution and cell survival.[9)] Although HSPs have been predominantly studied in heat stress, very few have focused on mechanical stress.

AlphaB-crystallin, one of the small HSPs, is reduced in the soleus muscle in rats that have release from mechanical stress by a hind-limb-suspension.[10)] The level of αB-crystallin was maintained or increased if the soleus muscle was stretched under non-weight bearing (hind-limb-suspension) conditions.[11,12)] αB-crystallin localizes in the Z band of striated sarcomeres.[10)] Z band corresponds to FA of the cell. Z-band is wider in a slow-twitch muscle cell. Soleus muscle is mainly composed of slow-twitch muscle. Cells have cytoskeleton and FA which correspond to pillar and fulcrum to exert a traction force at FA.[13)] More than 180 proteins are involved in FA.[14)] One of the better characterized proteins involved in FA, vinculin, is activated or inactivated as a result of changes in its configuration[15)] we speculate αB-crystallin might contribute as it's molecular chaperon.

Cells altered their orientation in response to stretch stress; in particular, endothelial cells changed their direction to near vertical to the stretch direction.[16)] However, when the stretch rate was increased or the stretch time extended, the cells detached from the chamber.[17)] In this study, we examined the mechanism by which HSPs, particularly αB-crystallin/HSPB5, assist FA adaptation during mechanical stress. Using soft and cell-stretchable styrene–(ethylene/butylene)–styrene block co-polymer SEBS[18,19)] sheet chambers, we were able to study the protective role of αB-crystallin in response to stretch stress to FA using vinculin as a marker as long as 78 h at 20% stretch rate.

2. Experimental methods

2.1. Cell stretching and cell lines

The Mechanical Cell Stretch System, "ShellPa" (Menicon Co., Ltd.),[20)] in a polydimethylsiloxane (PDMS) chamber with 2 cm × 2 cm SEBS sheet (SC4Ha, Menicon Co., Ltd.), was used in this experiment (Fig. 1). The L6 rat skeletal myoblast cell line was obtained from the American Type Culture Collection. The L6-KD cells (αB-crystallin protein expression level is 0.38 times that of wild type) and the L6-OE (αB-crystallin protein expression level is 2.33 times that of wild type) cells were prepared as previously reported.[21)] Before cell culture, the chamber was washed twice with PBS and once with cell culture medium. A total of 30 000 cells were seeded for both L6 and L6-KD, while 120 000 cells were seeded for L6-OE. More L6-OE cells were seeded to compensate for the cell lines slow growth rate.[21)] The cells were cultured overnight at 37 °C before stretching. We used a stretch frequency of 1 Hz to mimic the natural stress associate with the human heart, 1 Hz is often used in experiments.[22,23)] In our protocol, we used a 10 min incremental load method (2%, 4%, 5%, 6%, 8%, 10%, 12%, 15%, 20% at 1 Hz) to avoid detaching the cells from the SEBS sheet before reaching maximal stretch (20%) for longer periods (maximum 78 h) (Fig. 1).

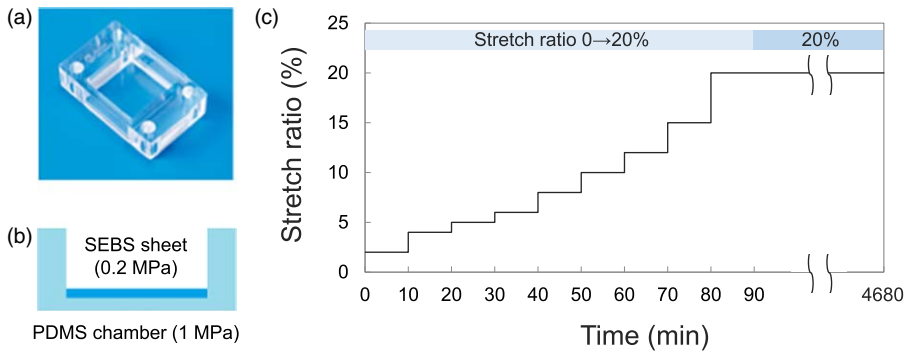

Fig. 1. (Color online) Stretch chamber with soft cell adhesive SEBS sheet used in this study. (a) The stretch chamber made from silicone. (b) The cell adhesion SEBS sheet was adhered to a silicon stretch chamber using excimer UV. (c) Overview of the cell stretch protocol used in this study. Initial stepwise 10 min incremental load method (2%, 4%, 5%, 6%, 8%, 10%, 12%, 15%, 20%) was used before stretching the cells with a constant 20% amplitude for 78 h.

2.2. Microscope observation of the live cells

Bright-field images were acquired using a microscope (Nikon ECLIPSE Ti) equipped with a CCD camera (DS-Fi2-U3, Nikon Co.) and Plan Apo 4× or 10× magnification. Images were analyzed using the NIS-Elements software (Nikon Co.).

2.3. Cell and nucleus rotation angle determination

To determine the cell and nucleus rotational angle, five points were struck to the contour of the cell and an elliptical approximation was drawn. Next, the inclination from the horizontal direction (direction perpendicular to the stretch direction) of the major axis of the ellipse was determined. The angle was determined to be in the range of 0°–90°. That is an angle of, 135°, 225° and 315° are the same as 45°. The cells that could not be elliptically approximated and the cells that overlapped were omitted. The direction of 100 cells was determined. Data are expressed as mean ± standard error of the mean (s.e.m.) for a given number of observations. For multiple group comparisons, either repeated-measure one-way ANOVA (Time-course experiments) or 2-way ANOVA (other experiments) was used to determine statistical significance. Post Hoc testing using the Holm analysis was employed when $p < 0.05$. All statistical analyses were performed using EZR (Saitama Medical Center, Jichi Medical University, Saitama, Japan), a graphical user interface for R (The R Foundation for Statistical Computing, Vienna, Austria). More precisely, it is a modified version of R commander designed to add statistical functions frequently used in biostatistics. The direction of the nucleus was examined in the same way and the roundness of the nucleus was also determined using the reciprocal of the aspect ratio.

2.4. Immunofluorescence study

For indirect immunofluorescence study, cells adhered to the stretch chamber were washed twice with Microtubule stabilizing buffer (MSB; 100 mM PIPES, 1 mM $MgCl_2$ and 1 mM EGTA, 2 M Glycerol), and soaked in MSBT (MSB + 0.5% Triton-X 100) for 10 s at 37 °C. Next, they were soaked in Fix2 (10% neutral buffered formalin supplemented with 2 mM $MgCl_2$, 2 mM EGTA, and 0.03% Triton-X 100) at 37 °C for 10 min. The cells were washed 3 times with PBS, soaked in blocking solution (1% BSA, 0.02% NaN_3 in PBS) and stored at 4 °C until antibody reaction. The following antibodies were used: Mouse monoclonal anti-vinculin (V9131, Merck), Rabbit anti-αB-crystallin (C-terminal) polyclonal antibody,[24] Goat anti-mouse secondary antibody, Alexa Fluor 546 conjugate (A11030, Invitrogen), Goat anti-rabbit secondary antibody, Alexa Fluor 488 conjugate (A11034, Invitrogen). Hoechst 33342, trihydrochloride trihydate, (H3570, Invitrogen) was used for DNA staining. Images were processed using a confocal laser scanning microscope (Nikon A1 RMP). Alexa Fluor 488 phalloidin (A12379, Invitrogen) was used for F-actin staining. All images were analyzed using NIS-Elements software.

2.5. Image analysis

All of the photographed images from this study were further analyzed using image analysis software ImageJ (NIH) to quantify the FA area using previously described methods.[23,25] Image processing was performed as follows. Image-Type-8-bit, Image Adjust-Threshold, Analyze–Analyze Particles (Size: 0–5 μm^2, Circularity: 0.00–1.00, Show: outlines, Display results). As it was difficult to draw a border between cells, the area and number in the FA analysis was calculated per field of view and then divided by the total number of cells as determined by Hoechst 33342 staining.

3. Results and discussion

3.1. Results

In this study we examined the roll of αB-crystallin in the maintenance of cellular adhesion during stretch stress. The cellular environment in the body is pliable, and the relative stiffness of the environment controls the mechanical response of cells. Young's modulus for soft tissue is in the range of 0.0105–20 MPa (Mechanical Property Database at http://cfd-duo.riken.go.jp/cbms-mp/). As a result, we used a PDMS chamber (1 MPa) with a soft 0.2 MPa SEBS sheet for adhesion in this study [Figs. 1(a), 1(b)]. To avoid cellular detachment from the stretch chamber, we used an initial stepwise 10 min incremental load method (2%, 4%, 5%, 6%, 8%, 10%, 12%, 15%, 20%) to acclimatize cells, and induce collagen synthesis,[26] before stretching them with a constant 20% amplitude (Fig. 1(c)]. Myoblasts already started to respond during the initial incremental load phase.

The cells were initially oriented randomly at average 45° before stretch (Fig. 2). When extended for a prolonged period, the cells direct to about 70° avoid stretch stress as in previous studies[21] (Fig. 2).

Cell angles were monitored over time (Fig. 3). Myoblasts were already affected by stretch stress in the initial incremental loading phase [stretch ratio 0% → 20% during initial 80 min in Figs. 1(c), 3]; however, the cell angle did not change with cell types until they started stretching at a

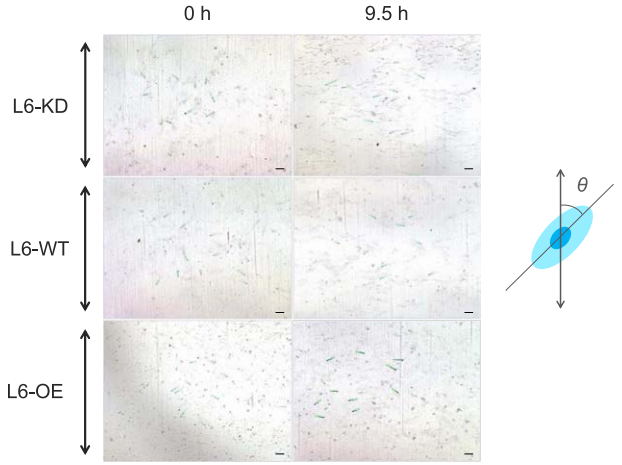

Fig. 2. (Color online) Images of cells before and after stretching. To determine the cell rotational angle, five points were struck to the contour of the cell and an elliptical approximation was drawn from the bright field microscope images. Next, the inclination from the horizontal direction (direction perpendicular to the stretch direction) of the major axis of the ellipse was determined. Representative an elliptical approximation of 10 cells at 0 and 9.5 h of 3 cell lines are shown. The scale bar represents 100 μm.

constant rate (stretch ration 20% after 80 min in Fig. 3). When repeated stretching was employed at a constant stretch rate of 20%, L6-KD cells with low αB-crystallin expression immediately lost stretch resistance and were vertically oriented to avoid stretching (Fig. 3).

To determine the cell orientation, nucleus angle was also used in the literature.[22] The cultured cells on the SEBS chamber with or without stretch was fixed, DNA was stained, and used for an elliptical approximation to determine the nucleus orientation to confirm the result obtained in Fig. 3 (Fig. 4). The cell angle of L6-KD cells, L6-WT cells, and L6-OE cells before stretching was not different among the three groups. The cell nucleus angles after 78 h were as follows: highly resistant L6-OE cells, 52.75° ± 25.12°, L6-WT cells, 63.17° ± 23.87°, and L6-KD cells, 73.99° ± 10.31°. The lower the expression of αB-crystallin, the closer was the cell orientation perpendicular to the stretch direction. The change in angle of the cell nucleus was also different among the three cell types after stretch stress (L6-KD versus L6-WT: $p < 0.01$; L6-WT versus L6-OE: $p < 0.01$; L6-KD versus L6-OE: $p < 0.001$) (Fig. 4). These results are consistent with the cell angle measurement (Fig. 3).

As the shape of the nucleus differs between cells, the circularity of the nucleus was also evaluated from the reciprocal of the aspect ratio. Before stretching, the nuclei of all three cell types showed significantly different roundness; 0.54 for L6-KD cells, 0.58 for L6 cells, and 0.68 for L6-OE cells. This showed that higher amounts of αB-crystallin caused rounder nuclei. Nuclei of L6-KD cells appeared rounder after stretching, while those of L6-WT cells and L6-OE cells remained the same as they were originally rounder than L6-KD cells. (Fig. 5).

Next, we evaluate the potential function of αB-crystallin in FA resilience. αB-crystallin and vinculin was visualized by immunostaining and found a partial co-localization after the stretch (Fig. 6). Only representative wild type image was shown here. When visualizing the area of FA of cellular vinculin on the SEBS sheet after stretching, the FA of L6-OE cells was particularly large (Fig. 7). F-actin (Fig. 7) and microtubules (data not shown) were oriented in the same way as the cells, as in previous studies.[27]

We counted the number of FAs and found that irrespective of differences in area of the FAs found in each group (0–1, 1–2, 2–3, 3–4, 4–5 μm^2), L6-OE cells had the highest number and largest areas of FA, indicating an improved FA induction in this cell line (Fig. 8).

3.2. Discussion

We conducted a stretch stress experiment in a stretch chamber using a soft cell adhesive SEBS sheet attached to a silicon chamber. [Figs. 1(a), 1(b)] Cells did not detach from the SEBS sheet under 20% stretch stress for an extended period (Fig. 2).

The angle of L6-OE cells (73.99°) after a 78 h stretch was close to that of the pennate muscle, where the muscle fibers were oriented obliquely. This is a characteristic observed in many slow muscle types, including the calf soleus and thigh muscle, which are bipennate to increase the cross-sectional

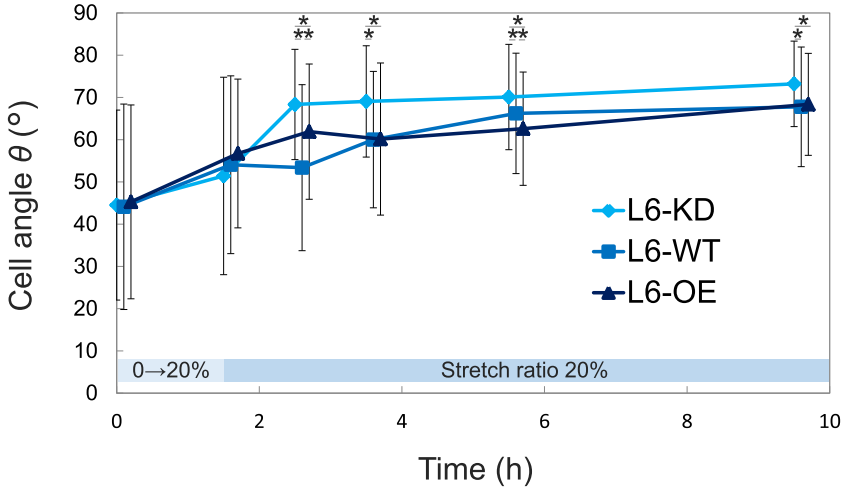

Fig. 3. (Color online) Change in cell angle. The direction of 100 cells was determined as in Fig. 2. Data are expressed as mean ± standard error of the mean (s.e.m.) for a given number of observations. For multiple group comparisons, either repeated-measure one-way ANOVA (Time-course experiments) or 2-way ANOVA (other experiments) was used to determine statistical significance. Relationship between extension time and cell angle are plotted. L6-KD cells could not withstand stretch stress and changed the cell angle early.

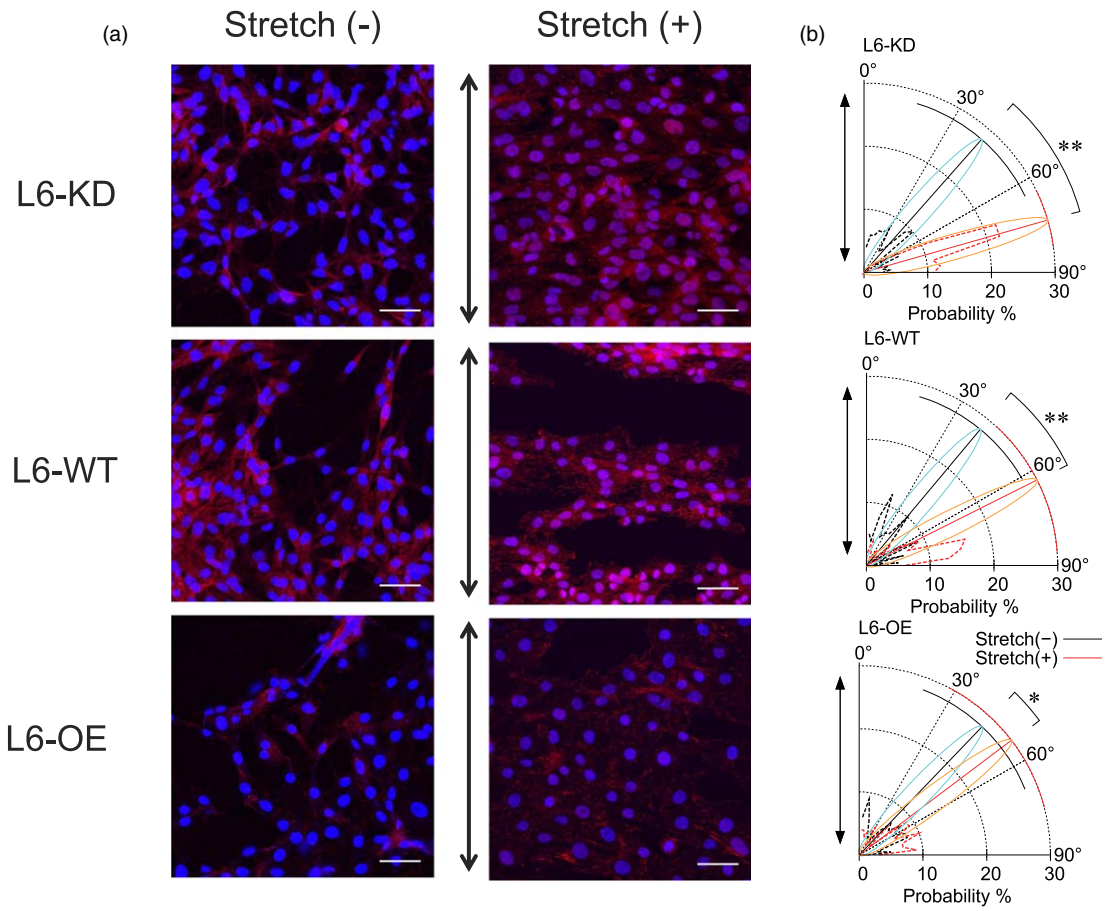

Fig. 4. (Color online) Change in the angle of the cell nucleus. (a) To determine the nucleus rotational angle, five points were struck to the contour of the cell and an elliptical approximation was drawn from the Hoechst33342 stained (for visualize DNA) cell confocal microscope images. Next, the inclination from the horizontal direction (direction perpendicular to the stretch direction) of the major axis of the ellipse was determined. (b) The direction of 100 cells was determined. Data are expressed as mean ± standard error of the mean (s.e.m.) for a given number of observations. For multiple group comparisons, either repeated-measure one-way ANOVA (Time-course experiments) or 2-way ANOVA (other experiments) was used to determine statistical significance. The cell nucleus angle was calculated before and after stretching and graphed. Lower amounts of αB-crystallin caused increased distance of the cell nucleus angle from the stretch direction. L6-KD cells appeared more sensitive to stretch stress. *: $p < 0.05$, **$p < 0.01$.

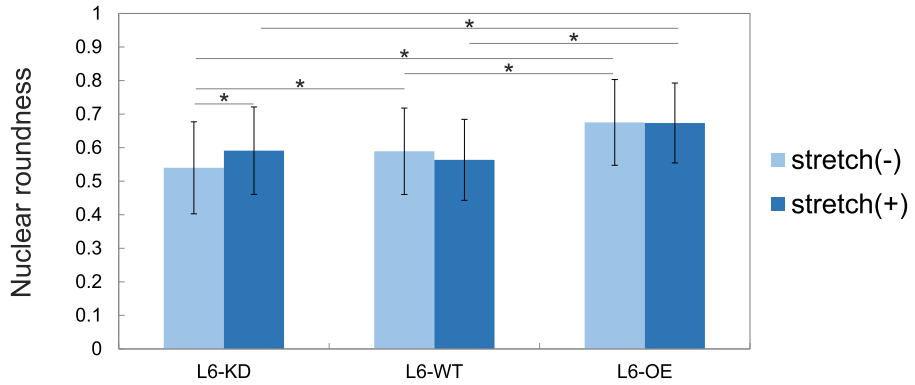

Fig. 5. (Color online) Roundness, reciprocal of aspect ratio, of cell nucleus before and after stretch. DNA was stained with Hoechst33342 and imaged with a laser confocal microscope. The nuclear roundness was analyzed by an image analysis software ImageJ (NIH). Greater amounts of αB-crystallin caused greater cell nucleus roundness before stretching, and less susceptibility to stretch stress. The nucleus of L6-KD cells became rounder than before stretching due to stretch stress. $N = 100$ for each cell line.

muscle mass. The L6 myoblast cell line was originally derived from the thigh muscle.[28] Although myoblasts fuse and differentiate into myotubes, it is possible that they may recognize the direction of elongation even in their singular cell form (myoblast) (Fig. 3).

L6-OE cells that overexpressed αB-crystallin persisted when subjected to stretch stress without turning perpendicular to the stretch compared to L6-KD cells (Figs. 3 and 4). Number and area of FA points in L6-OE cells was the largest among the three cell lines used in this study (Fig. 8). This evidence is consistent with our previous study which showed that reduction of FA dynamics leads to altered FA position and shape, and cells became motile. We showed that molecular chaperone αB-crystallin controls cell shape and adhesion stability under non-stress conditions in both glioma and myoblast cells.[21] αB-crystallin knockdown in both the

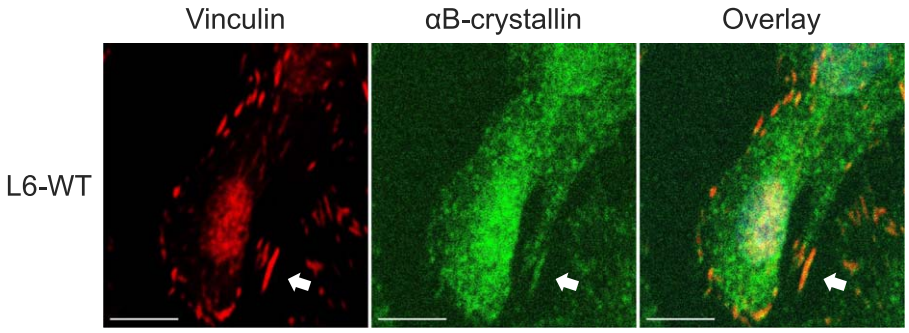

Fig. 6. (Color online) Co-localization of vinculin and αB-crystallin by immunostaining in fixed cells after stretching. Partial co-localization of vinculin (red) and αB-crystallin (green) was observed as shown by the arrow after the stretch. The images were taken in a sparse region in a stretch chamber for clarity. The scale bar represents 10 μm.

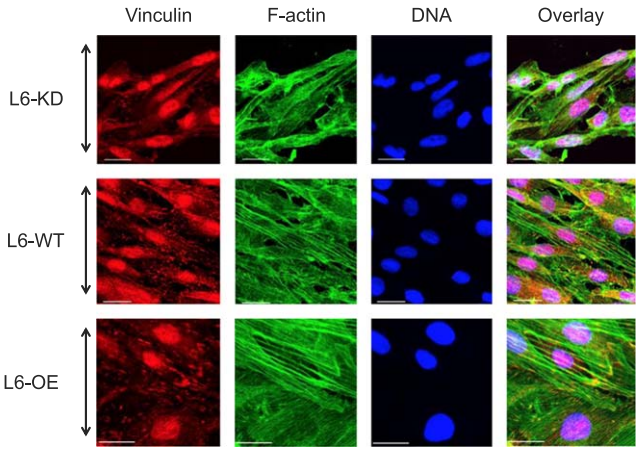

Fig. 7. (Color online) Immunostaining image in cells fixed after stretching. Vinculin staining in the first column represents FA. When stretch stress was continuously applied to the cells, FA increased in all cell types after 78 h, but the magnitude varied depending on the amount of αB-crystallin. F-actin was also oriented in the same direction as the cells (second column). DNA staining (third column) and overlay image of the three cell types (fourth column). The arrow is the direction of the stretch. Scale bar represents 20 μm.

C6 glial cells (αB-crystallin protein expression level is 0.11 times that of wild type) and L6 myoblast cells (0.38 times that of wild type) permitted both cell types to migrate more rapidly. Overexpression of αB-crystallin in cells led to an immortal phenotype as a result of persistent adhesion (1.84 and 2.33 times that of wild type C6 and L6, respectively). The position of matured FA, as visualized by vinculin immunostaining showed that stress fiber direction, length, and density were all demonstrably αB-crystallin dependent. All the results obtained in this study in addition to previous reports support the hypothesis that αB-crystallin functions in the soleus muscle of rats and supports its dynamic stability.

In L6-KD cells, cells are rod-like shape before the stretch and since L6-KD cells cannot expand their area unless they can extrude the microtubules, the nuclei of L6-KD cells are long even in the absence of stress (Fig. 5). In response, the roundness of the nucleus may change before and after stretch stress by the remaining αB-crystallin. Nuclear shape may also under control of αB-crystallin (Fig. 5) through tubulin/microtubules-FA axis and intermediate filament of vimentin-nuclear lamin axis, because αB-crystallin is a chaperone for free form of three cytoskeletal proteins of actin, tubulin and intermediate filament.[29–31] Nuclear skeletal lamin is a member of intermediate filaments, and overexpression of αB-crystallin protects the heart in dilated cardiomyopathy, and αB-crystallin protects lamin by heat stress on myoblasts,[32] there is a possibility that αB-crystallin contributed to the stability of lamin from stretch stress.

αB-crystallin has been previously shown to interact with tubulin in the cytoskeleton;[24] our study suggests that its interaction extends beyond the cytoskeleton and that it may be vital to the dynamics of FA. Co-localization was observed in the immunostained images of αB-crystallin and vinculin, which suggests a possible interaction either directly or

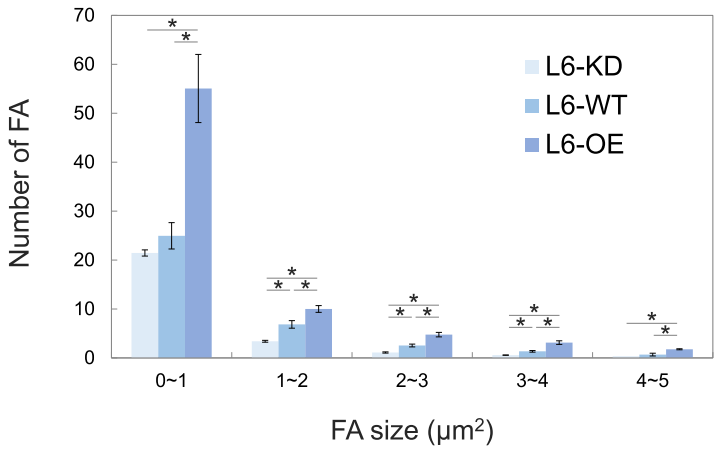

Fig. 8. (Color online) Various FA sizes in cells at 78 h after 20% stretch. As shown in Figs. 6 and 7, FA was visualized by vinculin staining and the FA area was determined by ImageJ software. The larger the αB-crystallin, the larger the FA after the 78 h stretch.

indirectly with unknown mechanism (Fig. 6). In L6-OE cells before the stretch, cells had a non-polarized round shape[21] and the FA vinculin area was the largest compared to other cell types (Fig. 8). This may explain the expression of αB-crystallin contributes to wider Z-band in soleus muscle. AF turnover is known to be regulated by microtubule dynamics.[33] αB-crystallin may dynamically maintain both FA as well as tubulin/microtubules.[24] Since vinculin changes its conformation during each step of FA development,[15] αB-crystallin as a molecular chaperon may necessary for its protein quality control. Further research should be directed towards similar stretch experiments using αB-crystallin complete knockout cells to test if the cells will be completely non-resistant to stretch stress, detach from the substrate, and do not survive.

4. Conclusions

The role of the molecular chaperone αB-crystallin in the control of cellular adhesion dynamics through interaction with vinculin was evaluated using a soft stretch system. We were able to show that αB-crystallin in myoblast cells contributes FA stability during stretch stress.

Acknowledgments

We thank Prof. K. Misawa (TUAT) for use of their laser scanning microscope.

ORCID iDs

Yoriko Atomi https://orcid.org/0000-0003-3808-6543

1) A. D. Doyle and K. M. Yamada, Nature **466**, 192 (2010).
2) S. McCue, D. Dajnowiec, F. Xu, M. Zhang, M. R. Jackson, and B. L. Langille, Circ. Res. **98**, 939 (2006).
3) J. Gao, X. Sun, T. W. White, N. A. Delamere, and R. T. Mathias, Biophys. J. **109**, 1830 (2015).
4) H. Kang, M. Liu, Y. Fan, and X. Deng, Astrobiology **13**, 626 (2013).
5) Y. Lu, Q. Zhao, Y. Liu, L. Zhang, D. Li, Z. Zhu, X. Gan, and H. Yu, J. Biomech. **71**, 67 (2018).
6) M. E. Feder and G. E. Hofmann, Annu. Rev. Physiol. **61**, 243 (1999).
7) H. Saibil, Nat. Rev. Mol. Cell Biol. **14**, 630 (2013).
8) M. M. Wilhelmus, W. C. Boelens, I. Otte-Holler, B. Kamps, R. M. de Waal, and M. M. Verbeek, Brain Res. **1089**, 67 (2006).
9) C. Queitsch, T. A. Sangster, and S. Lindquist, Nature **417**, 618 (2002).
10) Y. Atomi, S. Yamada, R. Strohman, and Y. Nonomura, J. Biochem. **110**, 812 (1991).
11) Y. Atomi, S. Yamada, and T. Nishida, Biochem. Biophys. Res. Commun. **181**, 1323 (1991).
12) T. Sakurai, Y. Fujita, E. Ohto, A. Oguro, and Y. Atomi, FASEB J. **19**, 1199 (2005).
13) L. Trichet, J. Le Digabel, R. J. Hawkins, S. R. Vedula, M. Gupta, C. Ribrault, P. Hersen, R. Voituriez, and B. Ladoux, Proc. Natl. Acad. Sci. USA **109**, 6933 (2012).
14) R. Zaidel-Bar and B. Geiger, J. Cell Sci. **123**, 1385 (2010).
15) H. Chen, D. M. Cohen, D. M. Choudhury, N. Kioka, and S. W. Craig, J. Cell Biol. **169**, 459 (2005).
16) K. Naruse, T. Yamada, and M. Sokabe, Am. J. Physiol. **274**, H1532 (1998).
17) S. Hong, H. Li, D. Wu, B. Li, C. Liu, W. Guo, J. Min, M. Hu, Y. Zhao, and Q. Yang, Mol. Med. Rep. **12**, 5342 (2015).
18) K. Langfeld, A. Wilke, A. Sut, S. Greiser, B. Ulmer, V. Andrievici, P. Limbach, M. Bastian, and B. Schartel, J. Fire Sci. **33**, 157 (2015).
19) M. D. Guillemette, E. Roy, F. A. Auger, and T. Veres, Acta Biomater. **7**, 2492 (2011).
20) J. G. Wang, M. Miyazu, P. Xiang, S. N. Li, M. Sokabe, and K. Naruse, Life Sci. **76**, 2817 (2005).
21) M. Shimizu, M. Tanaka, and Y. Atomi, PLoS One **11**, e0168136 (2016).
22) A. Salameh, A. Wustmann, S. Karl, K. Blanke, D. Apel, D. Rojas-Gomez, H. Franke, F. W. Mohr, J. Janousek, and S. Dhein, Circ. Res. **106**, 1592 (2010).
23) W.-H. Tsai, Comput. Vis. Graph. Image Process. **29**, 377 (1985).
24) Y. Fujita, E. Ohto, E. Katayama, and Y. Atomi, J. Cell Sci. **117**, 1719 (2004).
25) J. Wang, S. Sugita, K. Nagayama, and T. Matsumoto, Seitaiikogaku **53**, 311 (2015) [in Japanese].
26) J. B. Schmidt, K. Chen, and R. T. Tranquillo, Cell. Mol. Bioeng. **9**, 55 (2016).
27) M. Morioka, H. Parameswaran, K. Naruse, M. Kondo, M. Sokabe, Y. Hasegawa, B. Suki, and S. Ito, PLoS One **6**, e26384 (2011).
28) D. Yaffe, Proc. Natl. Acad. Sci. USA **61**, 477 (1968).
29) R. A. Quinlan and R. J. Ellis, Philos. Trans. R. Soc. London B **368**, 20130091 (2013).
30) Y. Atomi, M. Shimizu, E. Ohto-Fujita, A. Atomi, S. Hayasaki, Y. Higashi, and T. Atomi, in *Regulation of Heat Shock Protein Responses*, ed. A. Asea and P. Kaur (Springer, Berlin, 2018) Vol. 13, p. 307.
31) Z. Galata, I. Kloukina, I. Kostavasili, A. Varela, C. H. Davos, M. Makridakis, G. Bonne, and Y. Capetanaki, J Mol. Cell. Cardiol. **125**, 73 (2018).
32) A. S. Adhikari, K. Sridhar Rao, N. Rangaraj, V. K. Parnaik, and C. Mohan Rao, Exp. Cell. Res. **299**, 393 (2004).
33) S. J. Stehbens, M. Paszek, H. Pemble, A. Ettinger, S. Gierke, and T. Wittmann, Nat. Cell Biol. **16**, 561 (2014).